Chapter 3

Molecular Beam Deposition

In this research, the $CuIn_{1-x}Ga_xSe_2$ polycrystalline thin films used as an absorber layer in solar cells were fabricated using the molecular beam deposition (MBD) technique based on the equipment in the MBE system. This chapter describes the MBE physics and techniques based on the MBE system (EIKO model EW-100) but most general principles are also applicable to other systems. The preparation of the MBE system, substrate preparation procedure, as well as effusion-cell characteristics and calibration are also discussed in this chapter.

3.1   Overview of Molecular Beam Epitaxy

Molecular Beam Epitaxy (MBE) is one of the techniques for deposition of semiconductor materials developed in early 70s [44]. "Molecular Beam" is the term that describes a unidirectional flow of atoms or molecules of elements of which the film is composed. "Epitaxy" is the word used to describe the growth of one crystalline layer upon another crystalline layer. To obtain the unidirectional flow of atoms or molecules, the ultrahigh vacuum ($\approx 10^{-10}$ Torr) and the clean system environment are required for MBE growth.

The molecular beam condition, that the mean free path of the particles should be larger than the geometrical size of the chamber, is easily fulfilled if the total pressure does not exceed 10^{-5} Torr. Also, the condition for growing a sufficiently clean epitaxial layer must be satisfied, e.g. requiring that $t_{res} < 10^{-5} t_b$, where t_b is the monolayer deposition times of the beams and the t_{res} is the background residual vapor. Thus, ultra high vacuum (UHV) is the essential environment for MBE. Therefore, the desorption of gasous from the materials in the chamber has to be as low as possible. Pyrolytic boron nitride (PBN) is the material chosen for the crucibles which give low

rate of gas evolution and chemical stability up to $1400°C$. Molybdenum and tantalum are widely used for the shutters, the heaters and other components, and only ultra pure materials are used as evaporation source.

To reach UHV condition, a bake out of the whole chamber at approximately $200°C$ for 12 hr is required after the system is vented to the atmospheric pressure for maintenance. A water shroud around the chamber minimizes spurious fluxes of atoms and molecules from the wall of the chamber.

3.2   Basic Physical Mechanism of MBE Growth

The MBE system is carried out at pressure 10^{-9} Torr to 10^{-10} Torr. At this pressure level, the mean free path of the gas (λ) in the system is much larger than its dimensions, and can be estimated as [45]

$$\lambda = \frac{k_B T'}{\sqrt{2}\pi\rho^2 P} = \frac{1}{\sqrt{2}\pi\rho^2 N^*},\qquad(3.1)$$

where ρ is the collision diameter of the molecule, P is the pressure, T' is the temperature and N^* is the molar density.

When the effusion cell has a small orifice and is maintained at a temperature T (K), the vapor pressure p Torr of a source material inside the crucible should be equal to its equilibrium pressure. The total number (atom/sec) of atoms coming out through the orifice with area A (cm^2) is given by

$$\Gamma = \frac{pAN}{(2\pi MRT)^{1/2}} = 3.51\times10^{22}\frac{pA}{(MT)^{1/2}}\quad(molecules/sec).\qquad(3.2)$$

Here M is the atomic or molecular weight (g), N is Avogadro's number and R is the gas constant. From this it is possible to estimate the particle flux as

$$\Gamma = \int \vec{J}\cdot d\vec{A} .\qquad(3.3)$$

Ideally, the flux should be of spherical symmetry and this only depends on the distance from the cell orifice r. Under these conditions, the flux is expressed as

$$\bar{J} = \frac{\Gamma \bar{r}}{\pi r^3} .$$

(3.4)

If the distance to the substrate from the cell orifice L is sufficiently large compared to the substrate's diameter, one can assume the flux to be essentially the same for all points of the substrate. Thus we can write [46]

$$J_L = \frac{\Gamma}{\pi L^2} = \frac{pAN}{\pi L^2 (2\pi MRT)^{1/2}} ,$$

(3.5)

$$J_L = \frac{\Gamma}{\pi L^2} = \frac{1.118 \times 10^{22} pA}{L^2 (MT)^{1/2}} \quad (\text{molecules/cm}^2 \text{ sec}).$$

(3.6)

This equation indicates that the radial flux J_L of a molecular beam is proportional to A and p, and is inversely proportional to L^2.

3.3 The Molecular Beam Epitaxy (MBE) System

The MBE system (EIKO model EW100) at Semiconductor Physics Research Laboratory (SPRL), Department of Physics, Chulalongkorn University has been completely installed in the early of 2004. The system consists of two vacuum chambers; the load lock chamber and the main growth chamber, together with other supporting equipments, as shown in Fig. 3.1.

The load lock chamber is used to bring samples into and out of the main growth chamber through a gate valve on a flange with diameter of 8 inches. A magnetic coupler transfer rod is used to manually transport the sample between the load lock and the main growth chamber. Both of the main growth chamber and load lock chamber were pumped by a 1400L/s and 210L/s turbomolecular pump with each standard mechanical rotary pump, respectively. The special feature of this MBE system is that the system is cooled by water instead of conventional liquid nitrogen cool.
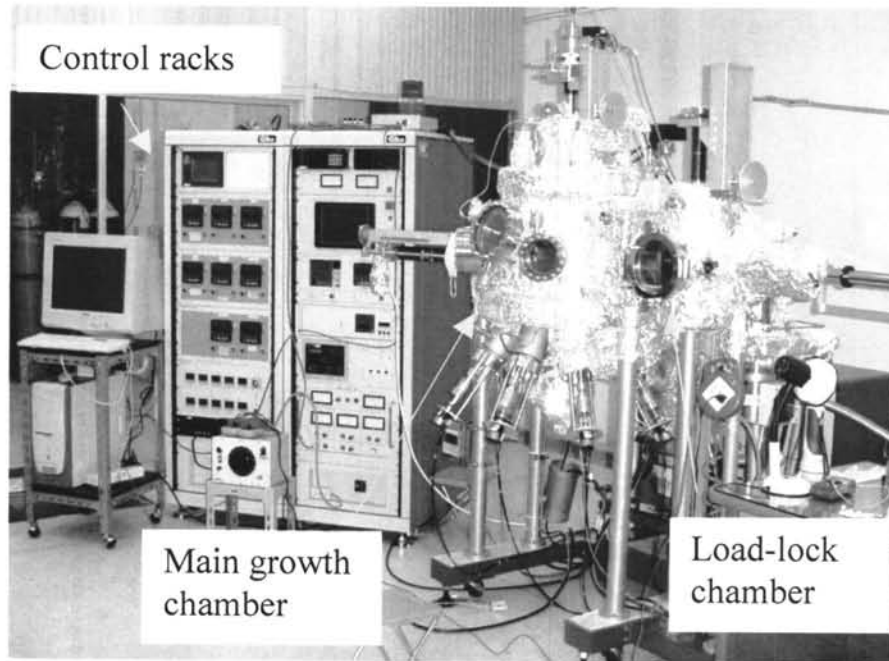
Fig 3.1: EW100 MBE system installed at the SPRL, Chulalongkorn University

3.3.1 The Main Growth Chamber

The growth facilities are contained within the main growth chamber such as Knudsen effusion cells for source materials, shutters, a substrate holder, beam flux ionization gauges, and *in situ* analysis equipments. There are four effusion cells installed at the bottom of the chamber. Each effusion cell consists of a Pyrolytic Boron Nitride (PBN) crucible and a heater is made of tantalum (Ta) wires. The crucibles are housed with Ta multi layer radiation shields. Each effusion cell is surrounded by a water-cool shroud, with individual thermocouple and shutter to prevent the interfere of the temperature. A PBN crucible can withstand temperature up to 1400°C. Above this temperature, BN may decompose and N_2 gas could be released. A conventional Knudsen cell (K-cell) is used for the Selenium (Se), Gallium (Ga), and Indium (In) sources. For the Copper (Cu) source, a dual-heater cell is used. It has a pair of electric feed-through providing currents to tantalum filaments along the body and the lip of the crucible which we can control the temperature of the two zones separately. Each effusion cell has a linear motion pneumatic shutter that controls the on-off state of the source beam. The transition time for open/close is less than 1 second. The shutter also

acts as a radiation shield which radiates heat back into the crucible. This causes a slightly higher source-temperature and thus a higher beam-flux at the initial growth stage after shutter opening.

During the growth process, each cell is independently heated until the desired flux of element material is achieved. We found that, in our system, changes in the temperature of as small as 0.5°C lead to changes of the material flux in the order of one percent. In order to control temperature variation to about 0.1%, highly stable control loops with Tungsten-Rhenium (W5%-W-Re26%) thermocouples and proportion-integral-deviation (PID) programmable temperature controllers are used. The computer controlled shutter are positioned in front of each effusion cells to stop the flux to reach the sample within a fraction of a second.

At the bottom of the growth chamber, we install a view port with a pyrometer which sits on the x-y stage slide table. The pyrometer points through view port toward the center of a substrate. This high resolution monochromatic (InGaAs, 1.55 μm) pyrometer (IR-FA model) is a fiber type radiation thermometer which has a measuring range of 250°C to 1000°C. Thus, it responds the infrared radiation from the surface of the heated substrate and determines the surface temperature from the emission wavelength.

A reflection high energy electron diffraction (RHEED) system is installed in the growth chamber to provide crystal structural information during growth process based on the diffraction patterns of electrons which are diffracted differently by periodic lattices.

A number of vacuum gauges provide vacuum pressure measurements in the main growth chamber. A nude ionization (Bayard-Alpert) gauge is used as a beam flux monitor (BFM) to measure the beam equivalent pressure (BEP) of element or the molecular flux reaching the substrate. We also use a quartz crystal thickness monitor (QCM) to calibrate the deposition rate. Both BFM and QCM are sitting on the translational arms that can be retracted away from the measurement position. A residual gas analyzer (RGA) provides another way of monitoring information about the residual molecules in the main growth chamber. It is also an efficient vacuum leak checking measurement.

3.3.2 The Load Lock Chamber

The load lock chamber is a vacuum chamber connected to the main growth chamber providing a rapid exchange mechanism for substrates into or out of the main growth chamber without breaking the vacuum in the main growth chamber. This can also reduce the risk of contamination in the main growth chamber. Our load lock chamber can house up to four substrate holders.

3.3.3 *In situ* Diagonostic Techinques

In this section, we will review the principle of various *in situ* analysis instruments installed in the main growth chamber such as beam flux monitor (BFM), residual gas analyzer (RGA), quartz crystal thickness monitor (QCM), reflection high energy electron diffraction (RHEED) and pyrometer, as the following.

3.3.3.1 Beam Flux Monitor (BFM)

One way to measure the molecular fluxes is to use the BFM to measure the beam equivalent pressure (BEP) of material sources. This measurement is dependent on factors such as the geometry of the system and ionization efficiency of the material being measured. The BEP reading is proportional to the flux at the sample surface and hence the growth rate. The flux (J_r) of a molecular beam is usually measured by placing a movable BFM in the substrate position. The pressure reading p_{BA} is proportional to the flux J_r and can be written as [47]

$$p_{BA} = J_r M v_{th} I(z) \infty J_r \sqrt{T_c M} \,, \tag{3.7}$$

where v_{th} is thermal velocity and $I(z)$ is the ionization coefficient of a material. $I(z)$ depends on the atomic number (z) of the materials with the expression [48]

$$I(z) = \frac{0.4z}{14} + 0.6 \,, \tag{3.8}$$

when compared with that of nitrogen.

For our MBE system, the upper limit of BEP reading is in the order of 10^{-5} Torr. However, there are several factors affecting BEP values. For example, the ion gauge can be severely interfered when the RGA unit is switched on. If sticking coefficients of species around the substrate holder are less than unity, desorbed atoms or molecules can also contribute to the measured BEP. While the Se flux is measured, the background BEP can reach as high as 10^{-7} Torr. At this stage it is inaccurate to measure BEPs from other material sources, because their BEP values are in the same range as the background. In our system, the main error of BEP readings was happened while the flux of Cu source was measuring. The heat radiation from the Cu K-cell including the flux of Cu atoms knock the metal grids of the BFM which were coated by Se overpressure during growth process, then causing the re-evaporation of Se atoms from the grids. This effect brings about the error of because the BEP reading because the reading is the sum of the BEP of Cu and Se knocked from the grids.

3.3.3.2 Residual Gas Analyzer (RGA)

The term "residual gas" refers to gases remaining in a vacuum system when the majority of the atmosphere previously occupying the vessel has been pumped out. The RGA is an application of the Quadrupole Mass Spectrometer (QMS). The mass spectrometers analyze charged particles called ion using either magnetic or electric fields to separate the ions of different masses. The data provided by the RGA can be qualitative (specifying the identity of the gases present), or quantitative (giving the partial pressure of each gas). In our system, the RGA is capable of determining gas composition in the range of $1 - 100$ AMU, with resolution of 0.5 AMU and partial pressure sensitivity of 10^{-12} Torr.

3.3.3.3 Quartz Crystal Thickness Monitor (QCM)

In principle, QCM utilizes the piezoelectric sensitivity of a quartz crystal monitor to added mass. The QCM uses this mass sensitivity to calculate the deposition rate and the final thickness of the deposited film. The QCM has a resonant quartz crystal with one surface exposed to the deposition sources. As a material is deposited onto the surface of the device, the resonant frequency changes because of

the added mass of the deposited film. The change in frequency of the crystal is compared to the reference frequency. The monitor then uses the known parameters of density and acoustic impedance of the source materials to determine the deposition rate and thickness.

The thickness of the film is evaluated from the change of the frequency of the quartz crystal, according to [49]

$$d = N_q \frac{\rho_q}{\rho_m} \left[\frac{\gamma_q - \gamma_2}{\gamma_2^2} - \frac{\gamma_q - \gamma_1}{\gamma_1^2} \right] \left(\frac{l_q}{l} \right)^2, \tag{3.9}$$

where d is the thickness of the deposited film,

ρ_q is the density of the quartz (2.20 gcm^{-3}) [50],

ρ_m is the density of the deposited film,

γ_q is the resonant frequency of the uncoated crystal (6MHz),

γ_1 is the resonant frequency of the crystal before the deposition,

γ_2 is the resonant frequency of the crystal after the deposition,

l_q is the distance between source and crystal,

l is the distance between source and substrate,

N_q is the frequency constant for a quartz crystal vibrating in the thickness

shear mode (1.668x10^{-5} cm/s) [51].

The Tooling-factor $\left(l_q / l \right)^2$ represents the different geometrical arrangement. In practice, the radiative heating of the quartz detector by the heat from the effusion cells must be minimized because the change of quartz temperature results in an erroneous reading. The replacement of the quartz is necessary for every 50 –100 μm thickness of deposited material.

3.3.3.4 Reflection High Energy Electron Diffraction (RHEED)

During the sample preparation it is important to monitor the *in situ* growth process in order to change the growth parameters if necessary to guarantee the high quality of the sample. The crystalline quality and the flatness of the epitaxial layers are of interest. RHEED is an *in situ* technique widely used for nondestructive method

to probe the surface crystal structure of the sample during the growth process. The ideal RHEED will be analyzed, assuming: (1) an incident electron beam which is monoenergetic, infinitesimally thin and collimated; (2) a very high beam energy such that the radius of the Ewald sphere is very large compared to the dimensions of the unit cell of the surface reciprocal net; (3) a small angle of incidence; and (4) a perfectly flat sample surface. Because of the small angle of incidence, RHEED is only sensitive to the uppermost atomic layers.
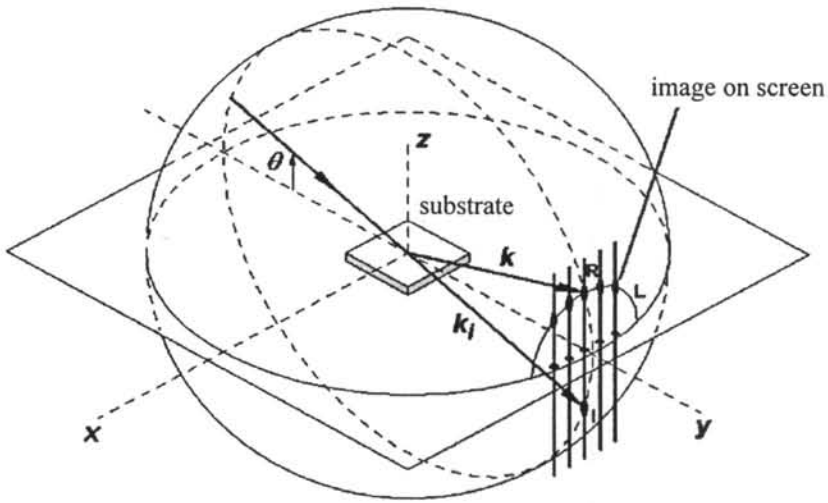

Figure 3.2: A schematic diagram of a RHEED measurement. The array of rods is the reciprocal lattice rods. Diffracted beams have maximum intensities when the Ewald sphere cuts the rods.

The basic principle of RHEED is similar to that of the X-ray diffraction. According to Bragg's law, the electron beam is diffracted at angle which satisfy

$$2d \sin\theta = \lambda,$$ (3.10)

where d is the lattice constant along the substrate normal, θ is the glazing angle of incidence electron beam and λ is the wavelength of electron beam which can be calculated from [52]

$$\lambda = \sqrt{\frac{150}{V(1+10^{-6}V)}} \; \text{Å},$$ (3.11)

where V is the high voltage applied on the RHEED-gun. An electron accelerating voltage ranging from 3 to 100 keV would correspond to wavelengths from 0.22 to 0.04 Å. Fig. 3.3 shows a plan view of a single row of rods with lateral spacing d*. The observed streak spacing is W and the distance to the screen from the point of incidence is L. The relation between the atomic arrangements on the substrate and the observed diffraction pattern on the fluorescent screen can be expressed as

$$\frac{W}{L} \approx \frac{a*}{(1/\lambda)}.$$ (3.12)

Thus, the observed streak spacing indicates a rod spacing of

$$a* = \frac{W}{\lambda L}.$$ (3.13)

Figure 3.3: A plan view showing the relation between the intra row spacing of the reciprocal lattice rods and the spacing of the observed RHEED streaks.

Figure 3.4(a) shows that the diffraction spots on the RHEED screen from a flat highly-ordered crystalline will appear along the Laue circles. When surface roughness is present in the sample the diffracted spots will elongate and turn into streaks normal to the surface (Fig. 3.4(b)), because the roughness introduces a broadening of the reciprocal lattice rods. If the sample roughness is further increased, the electrons transmitted to crystalline islands on the surface will give rise to a three-dimensional

diffraction pattern. This transmission pattern will change into spots as the height of the surface roughness increases as shown in Fig. 3.4(c). Finally, a polycrystalline surface (randomly oriented single crystals) will gives rise to ring patterns on the RHEED screen (Fig. 3.4(d)).
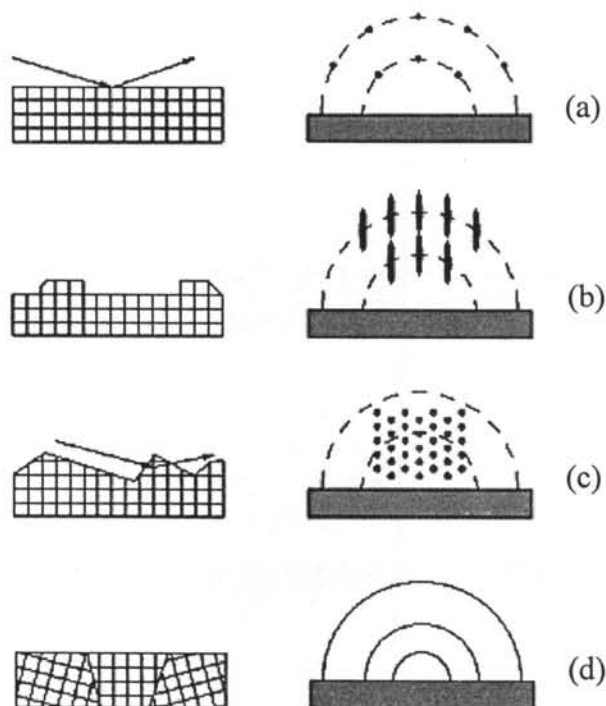

Figure 3.4: RHEED patterns from surfaces with different morphologies.

3.3.3.5 Pyrometer

The pyrometer is the radiation thermometer which converts the detected radiation intensity signal into a temperature, for a given emissivity and wavelength. Emissivity (E) is defined as the ratio of the energy radiated by an object at a given temperature to the energy emitted by a perfect radiator, or blackbody, at the same temperature. The emissivity of a blackbody is 1.0. All values of emissivity fall between 0.0 to 1.0. Reflectivity (R) is a measure of an object's ability to reflect infrared energy. Transmissivity (T) is a measure of an object's ability to transmit infrared energy. Both R and T are related to emissivity. All radiation energy must be either emitted (E) due to the temperature of the body, transmitted or reflected. The sum of emissivity, transmissivity and reflectivity, is equal to 1. Most objectives are

not perfect radiators, but will reflect and/or transmit a portion of the energy. The pyrometer also has the ability to compensate for different emissivity values, for different materials.

3.4   System Preparation and Characterization

In this section, we will describe the calibration of growth parameters in molecular beam deposition (MBD) growth process. As discussed before, the reduction of background impurity level is essential for growth of high quality films. Thus, we focus on minimizing background impurity incorporation in conventional steps such as pumping down, baking the MBE system, outgassing the crucibles, and calibrating substrate and flux of source materials.

3.4.1 Baking the MBE System

Once the MBE system is exposed to an atmosphere for more than 10 minutes or some new or repaired components are installed, it should be thoroughly cleaned. We usually pump the system down to below 10^{-8} Torr which can be reached for an overnight period. The typical baking period is about 12-15 hours. The bake-lamp heaters are permanently installed inside the main growth chamber. While the baking heater-tapes and heater-wires are attached to the outside of both main growth chamber and load lock chamber. These wires and tapes are wrapped around the flanges of K-cells, the transport rod. This will bring the temperature of main growth chamber at 150-200°C and that of the load lock chamber to be at 150°C during the baking.

During this process, the substrate heater is kept at 120°C to prevent adsorption of the gases desorbing from the hot walls on the substrate heater. Generally, baking for $12 - 15$ hours is enough for the pressure to reach around $6 - 7 \times 10^{-10}$Torr after the system is cooled down to room temperature. Then followed by the use of Titanium Sublimation Pump (TSP), the background pressure can eventually reach 2×10^{-10}Torr as shown in Fig. 3.5.
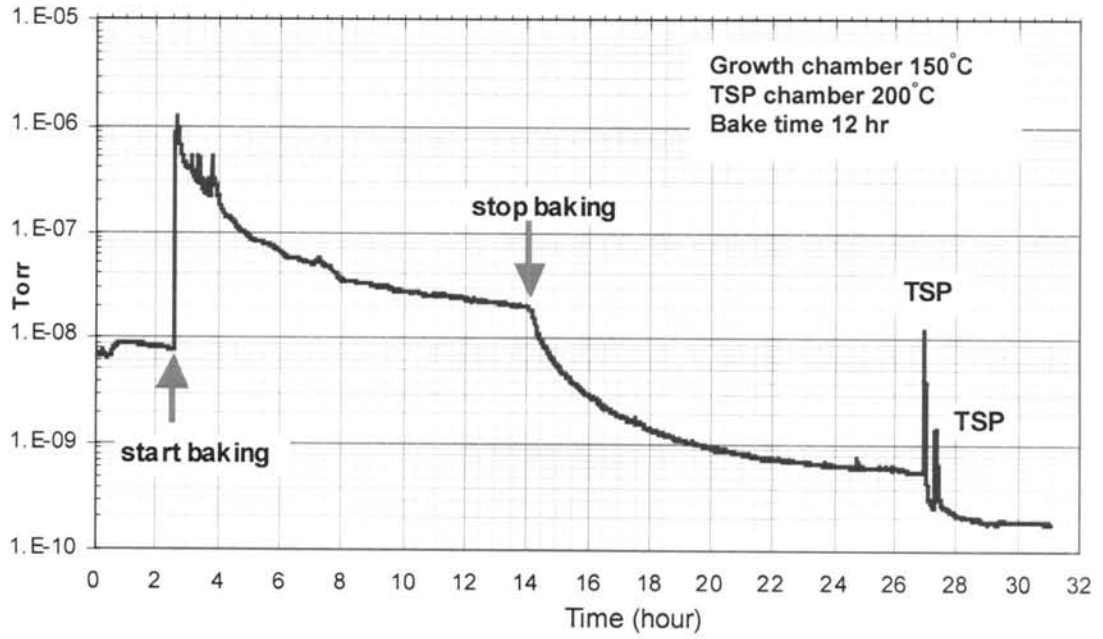
Figure 3.5: Pressure in the main growth chamber before and after the baking process.

3.4.2 Checking the Residual Gas Using the RGA

Species of gases found in the MBE system are summarized in Table 3.1.
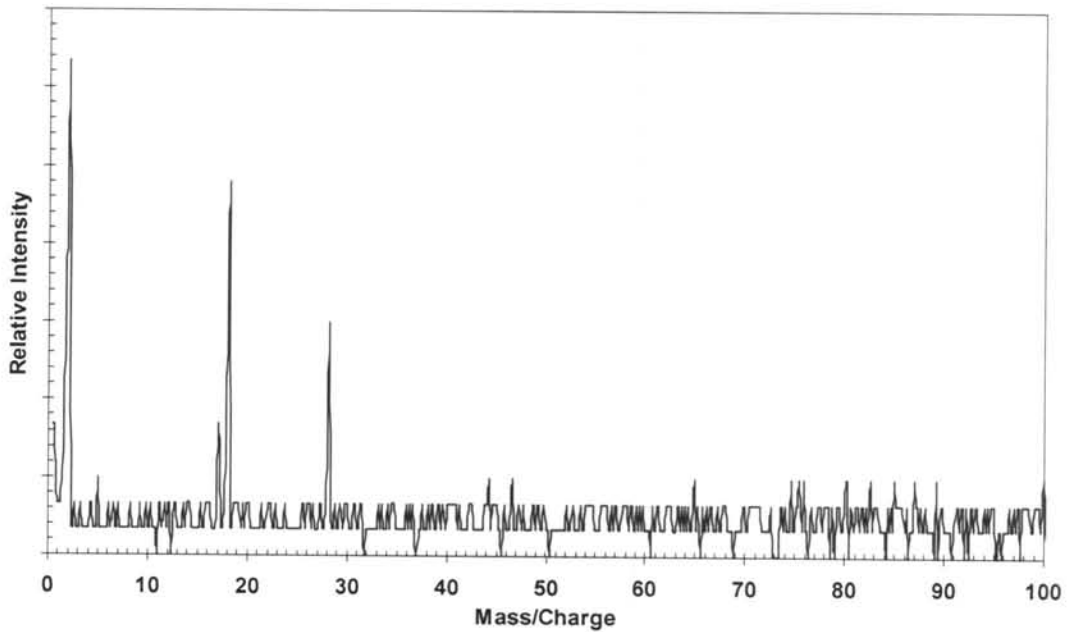

Figure 3.6: Mass/Charge spectrum obtained from the RGA at $P \approx 3 \times 10^{-10}$ Torr.

Table 3.1. List of possible species of gases found in the MBE chamber detected by a RGA. Some species are decomposed from stable gas molecules.

Mass/charge ratio	Suspected gas specie	Comments
2	Hydrogen	Hydrogen is often the major gas load in UHV systems due to permeation through stainless steel vessel walls. Dissociation of water and hydrocarbons may also give a peak at 2.
4	Helium	May be present following leak checking.
16	Oxygen	Singly ionized monatomic oxygen may be present due to dissociation of water, or from an air leak.
18	Water	In the high vacuum range, water vapor is the largest contributor to the gas load. If water is present peaks should also be seen at 16 and 17.
19	Fluorine	May indicate the decomposition of fluorinated hydrocarbons in the vessel.
20	Neon	May be observed in UHV systems with ion pumps
28	Nitrogen	Diatomic nitrogen, single ionized. If nitrogen is present, an air leak may be the cause. A peak at 14 for monatomic nitrogen, singly ionized should also be present.
28	Carbon monoxide	Resistively heated tungsten filaments emit significant amounts of CO. Turn off ion gauges to reduce this effect. Peaks for carbon and oxygen should be present.
30	Nitrous oxide	Another possible by-product from heated filaments within the vessel.
32	Oxygen	Diatomic oxygen, singly ionized. The presence of this specie may indicate an air leak, especially if a stronger peak at 28 (nitrogen) is observed.

Mass/charge ratio	Suspected gas specie	Comments
40	Argon	Argon may be present due to an air leak.
44	Carbon dioxide	May be generated from heated tungsten filaments, as with CO.
45	Isopropyl alcohol	May be a residue from a cleaning process used on a component in the vessel.
58	Acetone	See comments for isopropyl alcohol.
95	Trichloro-ethylene	See comments for isopropyl alcohol.

A typical mass/charge spectrum recorded using RGA after baking our main growth chamber is shown in Fig. 3.6. The background pressure is 3×10^{-10} Torr. The dominant peaks in a clean main growth chamber are mass/charge = 2, 17, 18, and 28, which correspond to H_2^+, H_2O^+, N_2^+, CO^+ and hydrocarbons. The RGA is also used as a high sensitivity leak detector. By monitoring the He^+ peak (mass/charge = 4), a small steady leak at 10^{-10} Torr can be detected.

3.4.3 Outgassing of Crucibles and Source Materials

This procedure is divided into three steps. The first step is to outgas the heaters of the effusion cells themselves with no PBN crucible installed. The second step is to bake the effusion cells with the empty crucibles installed, while the last step is to outgas loaded crucibles with source materials.

Before outgassing of newly loaded materials, each source is slowly heated to a temperature slightly above the maximum working temperature. The sources are baked at this temperature with close shutter for about 2-3 hours until the background pressure of main growth chamber reaches a stable value. We also use an RGA to monitor and record all gases that come out into the chamber before and after each

temperature ramp. This procedure is repeated for all sources used in the main growth chamber. After this step, the system is ready for deposition process.

3.5   Calibration of Growth Parameters

Calibration of growth parameters such as substrate temperature, and deposition rate should be done before growth process. In this section, we start with the preparation of substrates used in calibration process. Consequently, we will describe the substrate calibration and K-cells calibrations.

3.5.1 Substrate Cleaning Procedure

The substrate and precise control of the substrate temperature are one of the important factors to get high quality thin films. Moreover, a clean substrate surface is an important prerequisite for film growth both epitaxial and deposition. Since the contaminations from the atmosphere or other sources can easily contaminate the clean GaAs wafer and soda-lime glass substrates and eventually degrade the optical and electrical properties of as-grown film. In this section, we will describe how we prepare the soda-lime glass and GaAs substrates and how we calculate the substrate temperature.

3.5.1.1 Soda-lime Glass Cleaning Procedure

We use a 3x3 cm^2 (2mm thick) SLG as a substrate to grow polycrystalline CuIn$_{1-x}$Ga$_x$Se$_2$ thin films. Firstly, we manually clean the SLG substrates with commercially available glassware detergent, and follow by ultrasonic cleaning at 60°C for 30 minutes. Then we rinse the substrates with a lot of de-ionized (DI) water and blow dry with compress nitrogen gas. The clean substrates are generally stored in the dry cabinet to reduce contamination before deposition process.

The clean SLG substrates were coated with 0.4 µm thick of molybdenum film by DC magnetron sputtering for use as a back electrode in solar cell structure. The

SLG or Mo/SLG substrates are mounted on an In-pasted Mo block or In-free stainless steel block with sapphire diffuser. Sample holders with fresh substrates are then quickly loaded in the load lock chamber.

3.5.1.2 GaAs Wafer Cleaning Procedure

The cleaning process of GaAs involves removal contaminants from the surface and preparation of smooth surface of the GaAs wafer. In order to remove grease, organic compounds, dust and other contaminants from the surface, the GaAs substrates are thoroughly cleaned. The following steps are taken:

1. Rinse the substrate thoroughly in DI water to remove coarse dust particles.

2. Clean the substrate for 5 minutes in Trichloroethylene (TCE) in an ultrasonic bath to remove organic contamination that might be left on the surface from the substrate production.

3. Clean the substrate for 5 minutes in acetone in an ultrasonic bath to further remove organic contamination and residual TCE.

4. Clean the substrate for 5 minutes in methanol in an ultrasonic bath to further remove organic contamination and remaining acetone.

5. Thoroughly rinse in DI water to remove any residual methanol. Then blow dry with compress nitrogen gas. Degreasing process of GaAs wafer is complete.

6. Etch the GaAs wafer with etching solutions which consists of 98 weight percent sulfuric acid, 30 weight percent hydrogen peroxide, and DI water. The sulfuric acid converts organic compounds to elemental carbon. The peroxide then oxidizes the carbon to carbon dioxide and water. The temperature of the etchant several minutes after mixing is around 50°C.

7. Dip the wafer for 1 minutes in $H_2SO_4 : H_2O_2 : H_2O$ with the ratio 5 : 1 : 1 and agitating every 5 seconds to remove metal ions and to oxidize the surface.

8. Etching is stopped by rinse in running DI water for 2-3 minutes to remove $H_2SO_4 : H_2O_2$

9. Blow dry with purified nitrogen gas.

3.5.2 Calibration of Substrate Temperature

After finished the GaAs substrate cleaning procedure, the sample is mounted on the molybdenum sample holder (Mo block) by using a small amount of In solder. The Mo block is placed on the hot plate and kept at $160 - 180\,^{\circ}$C. By sliding a GaAs sample back and forth along with good thermal contact to the Mo block. It is important to wet the entire surface to ensure uniform heating and to prevent inclusion of gas between the wafer and the Mo block. After cooling down the sample, it is ready to be loaded into the load lock chamber. After growth, the wafer can be removed by reheating the block above the melting point of In.

In the main growth chamber, the Mo block is housed by the manipulator. The manipulator are one of the most complicated parts in the MBE system because it has many parts that can provide complex growth procedures such as a Tantalum heater providing heat to the substrate, a motor to rotate the substrate for uniformity during growth, vertical translation mechanism to adjust the height of the substrate, etc. The heater is powered by a PID temperature controller while the Tungsten-Rhenium thermocouple which is barely touch the backside of the Mo block is used to monitor the temperature providing the feedback to the PID controller. Since the Mo block is about 3 mm thick, and the gap between the thermocouple and the Mo block, the reading of the substrate temperature is not quite accurate. To solve this problem, we use a pyrometer to monitor the surface temperature of the sample. To obtain a correct reading temperature from the pyrometer, it must be calibrated with some known sample. We use the desorption temperature of a thin oxide layer (Ga_2O_3) formed on the surface of GaAs at $583\,^{\circ}$C [53] as the point for calibration by observing the RHEED pattern. This can provide the determination of the temperature difference between the thermocouple and the substrate's surface temperature.

Figure 3.7 shows the RHEED pattern before and after the desorption of the oxide layer on the GaAs wafer. At room temperature, before the desorption of the oxide layer, the RHEED observation shows a haze which is indicative of the amorphous nature of the protective oxide formed on the GaAs surface. The set point of the substrate heater temperature controller is ramped up slowly, the oxide gradually

desorbs, and amorphous ring pattern appears. When the oxides are almost desorbed, bright spotting pattern appear. As discussed above, the temperature of the substrate is monitored using the thermocouple above the back side of the Mo block while that of the surface of sample is monitored by the pyrometer. We also note that the de-oxidation temperature according to the thermocouple varies approximately by 20-50°C from one Mo block to another. The oxide desorption temperature which is being read by the pyrometer is about 160°C less than being read by the thermocouple. However, there are still some uncertainties with this method. The transition from hazy to clear diffraction pattern also depends on the temperature ramp rate and the nature of initial oxide. Thus, in typical growth process, after RHEED shows that the oxide has already been desorbed, the sample temperature is increased about 20°C for 5-10 minutes to ensure that all traces of the oxide are removed.

By setting the emissivity value used by the pyrometer to read 583°C at the desorption temperature of the oxide layer on the GaAs surface, we then also use the pyrometer as the main sensor to read the surface temperature when using the SLG as the substrate. In our system, the value of emissivity is 0.11.
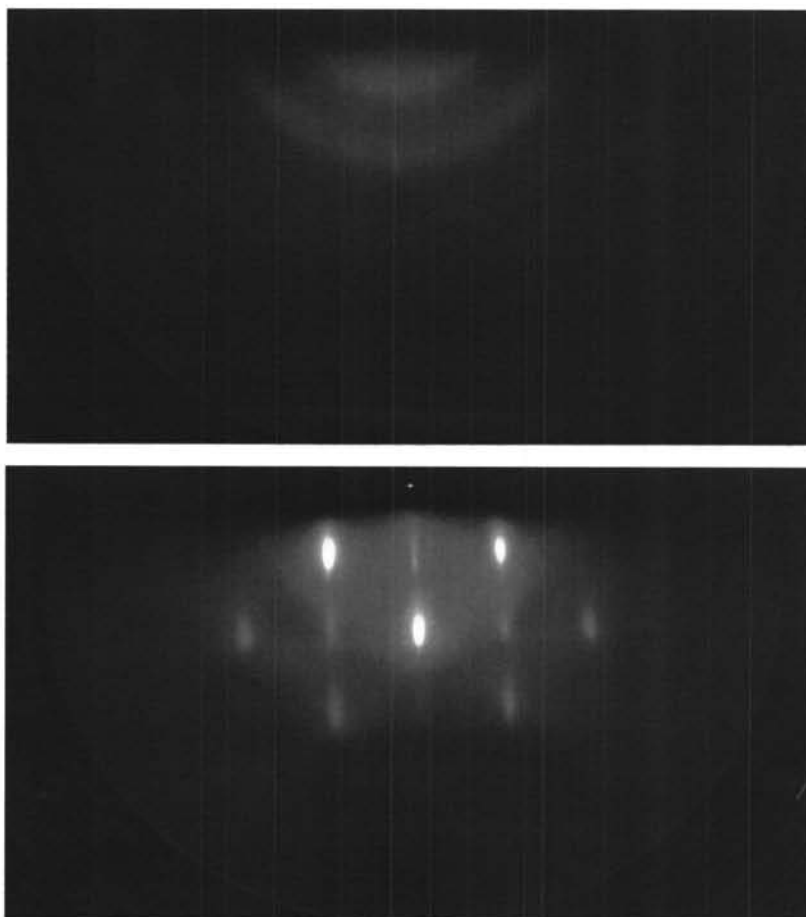
Figure 3.7: RHEED patterns from the GaAs surface (a) at room temperature showing amorphous oxide covering the surface, (b) at 583°C when the oxide layer is removed from the surface.

The comparison of the surface temperature of the SLG substrate reading from the pyrometer and the temperature setting at the PID controller is shown in Fig. 3.8. The calibration curve for the SLG substrate surface temperature versus the temperature set point showing a linear relationship is shown in Fig. 3.9.
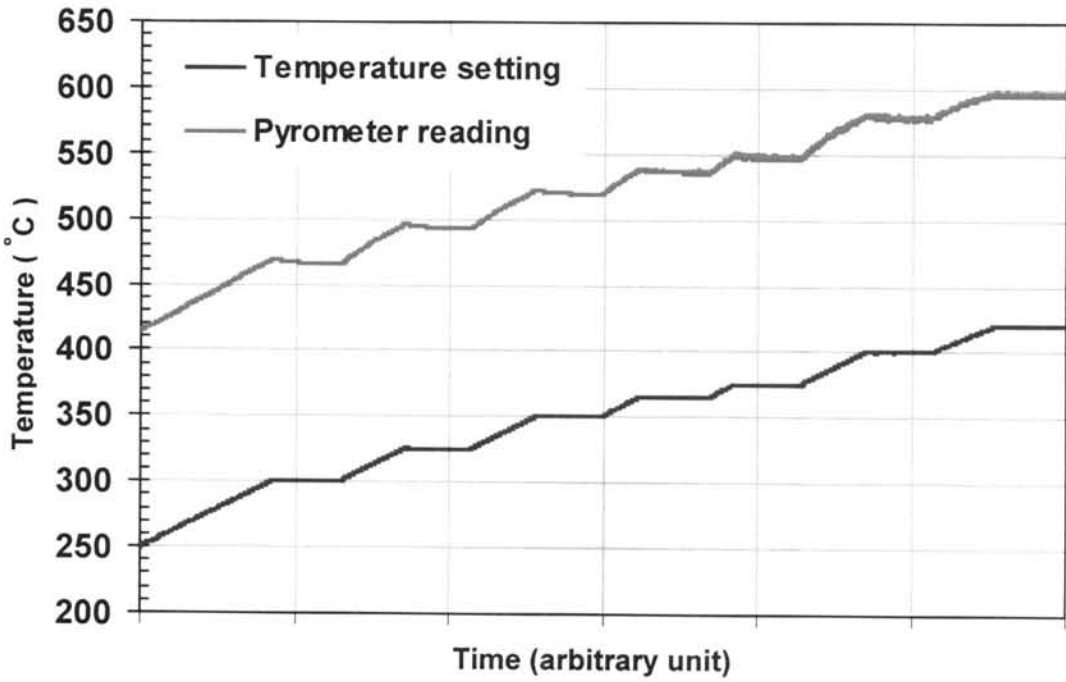
Figure 3.8: Comparison of the temperature profile reading from pyrometer and the PID controller setting.
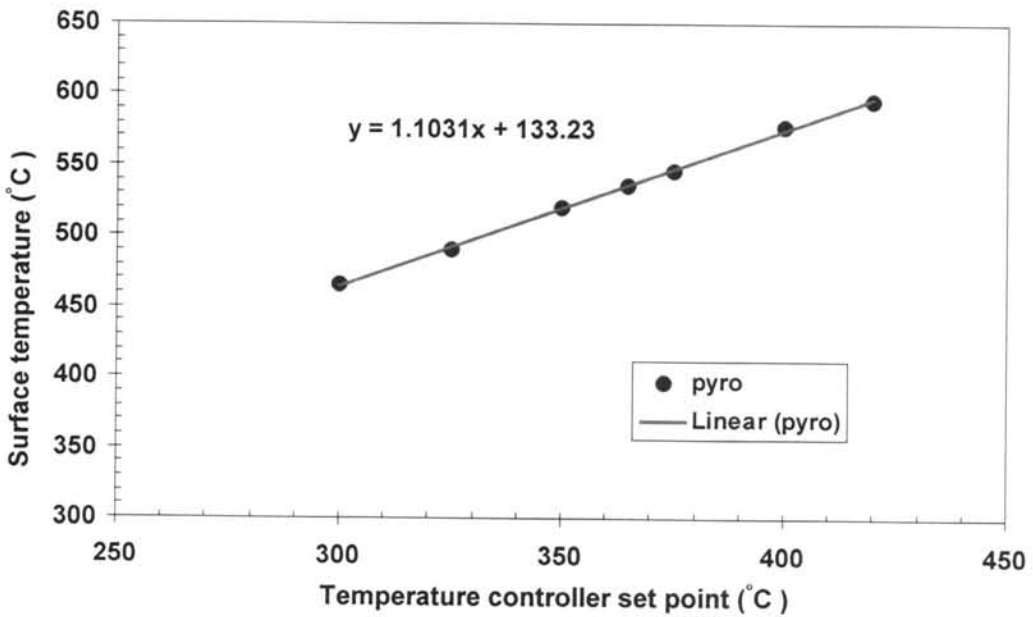

Figure 3.9: Calibration curve of the surface temperature of SLG versus PID controller setting.

As described in Section 3.4, the substrate holder used in MBE system is the In-pasted Mo block with thickness of 3 mm. The substrates were heated by heat conduction through the block. Because blocks are massive, the substrate temperature (thermocouple and pyrometer reading) are not possible to immediately response to the abrupt change in temperature profile of substrate in the three-stage growth process of polycrystalline $Cu(In,Ga)Se_2$ films. By using the In-pasted Mo block, after growth, the block as well as the substrate must be reheated above the melting point of In ($> 150\,^{\circ}C$) which may effect the surface of film. Moreover, the back side of the SLG gets rough and coated with In. Consequently, the sample ($Cu(In,Ga)Se_2$ /Mo/SLG) cannot be used in the solar cell fabrication process. Thus, it is necessary to modify the substrate holder to mount the Mo coated SLG substrate without In solder.

In our modified substrate holder as shown in Fig. 3.10, the Mo coated SLG substrates were heated by radiation from a heater through an unpolished sapphire heat-diffuser plate with minimal thermal contact to the holder.
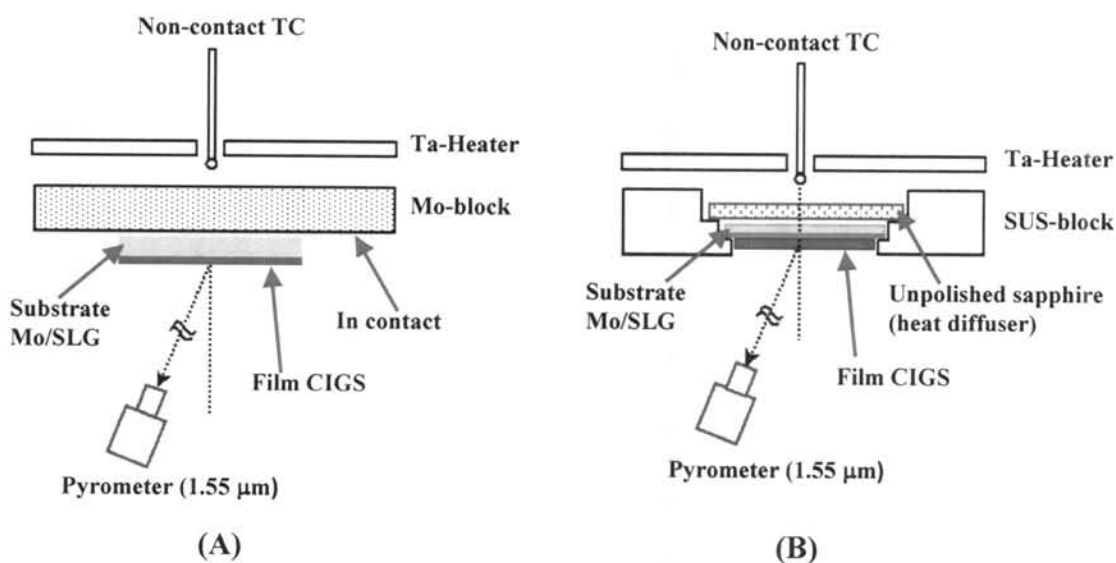

Figure 3.10: Schematic diagram of the arrangement of the substrate heater and the position of the pyrometer. The pyrometer was focused on the center of substrate. (A) Typical set-up and (B) modified set-up that the heat diffuser provided paste-free, uniform and reproducible heating of the substrate.

3.5.3 Calibration of Effusion Cells

Calibration of the effusion cells should be done periodically to check the effusion rates of various growth materials. The calibration is a measure of the flux and rate of atoms or molecules of the materials used as a function of the effusion cell temperature. The recorded value of the temperature of the effusion cell is the reading at temperature controller. The purity materials (Cu, In, Ga:6N, Se:5N) were evaporated from four effusion cells. The four effusion cells were independently controlled by programmable PID temperature controllers to emit appropriate fluxes of Cu, In, Ga and Se. The incident angles of all beams impinging on the substrate are designed to be about 15 degrees. In order to obtain the relation between effusion cell temperature and deposition rate, the Quartz Crystal Monitor (QCM) and the Beam Flux Monitor (BFM) which are located on the retractable arms under the substrate were used as follow:

1. Measuring the deposition rate using the crystal thickness monitor (QCM) and

2. Measuring the beam equivalent pressure (BEP) using the beam flux monitor in the line-of-sight to the source. The recorded value of the BEP is the pressure reading value when the shutter is open minus the reading value when the shutter is closed, as shown in Fig. 3.11-3.12.
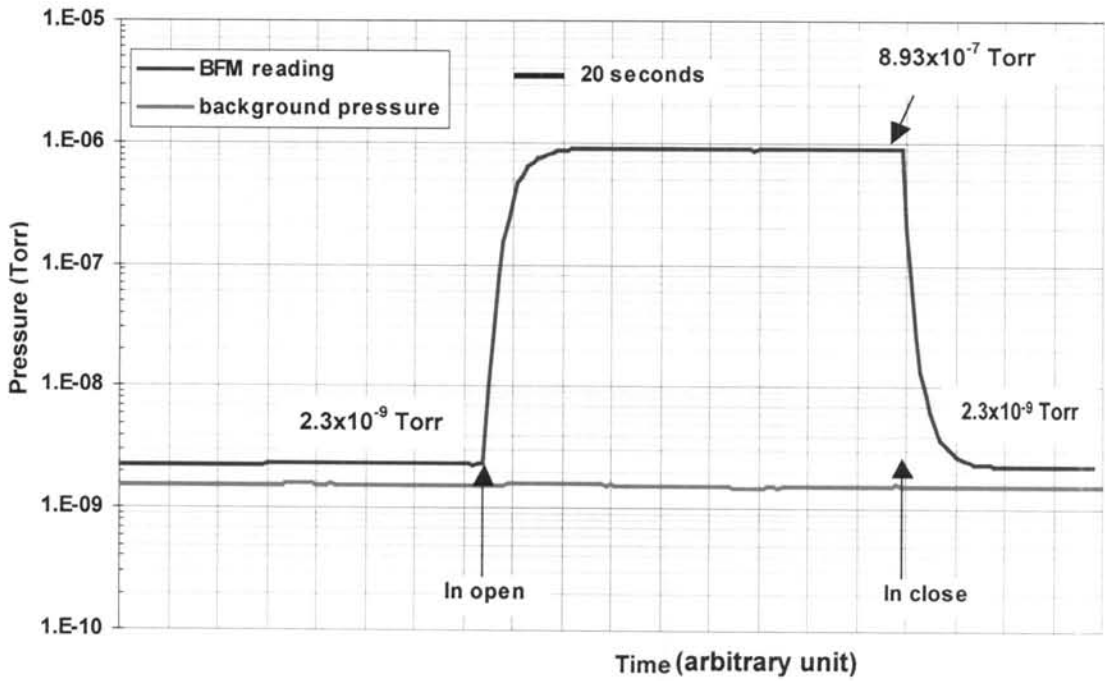
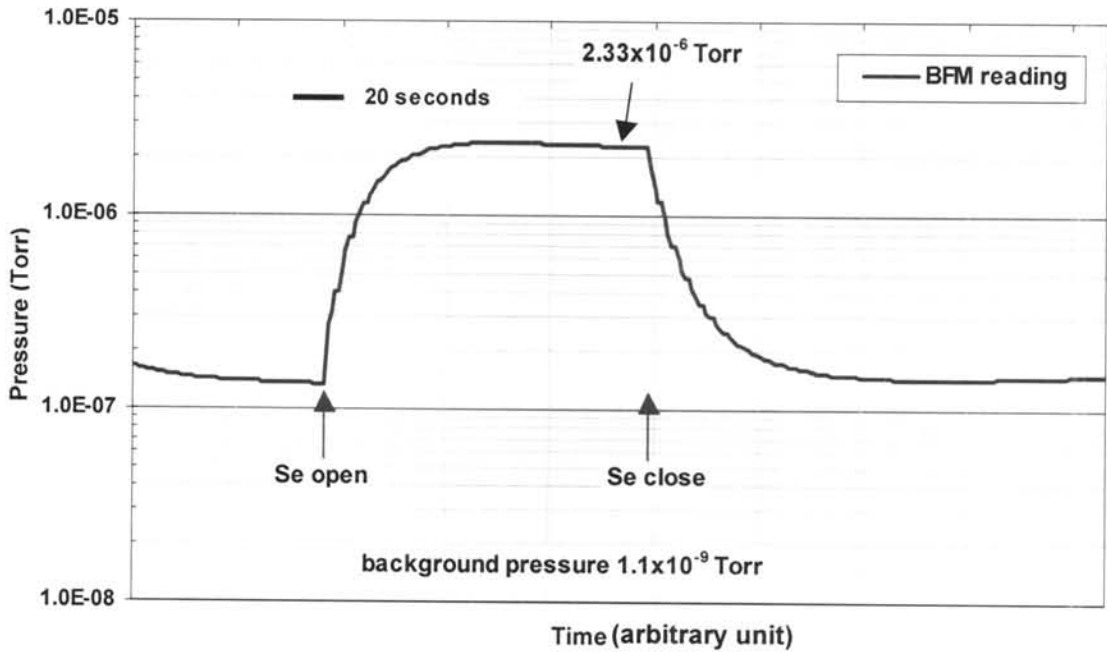**Figure 3.11:** Time response of the BEP for an In source.

Figure 3.12: Time response of the BEP for an Se source.

Beam flux ratio is obtained by measuring beam equivalent pressure (BEP) of elements. The typical BEP-curves versus time is shown in Fig. 3.11-3.12. The BEP of

Se rapidly increases in the beginning and then slowly increases to the equilibrium. The slow increase could be due to Se desoption from the areas around the ion gauge and consume longer than 45 seconds to reach an equilibrium value whereas, the BEP of metals rise shorter than 30 seconds to reach an equilibrium value.

To measure the deposition rate using the QCM, we usually open the shutter and wait for a few minutes before measuring due to an initial transient. Besides that, the deposition rate can be directly calculated an absolute number of elemental flux in unit of $1/(cm^2 \ s)$. The conversion factor is $(10^{-8} \cdot \rho \cdot N)/M$, where ρ is the density of element, N is the Avogadro number, and M is the molecular weight of element as summarized in Table 3.2.

Table 3.2: Flux conversion factor for source elements.

Element	Conversion factor ($1/cm^2$ s)
Cu	8.49×10^{14}
In	3.83×10^{14}
Ga	5.12×10^{14}
Se	3.65×10^{14}

For our MBE system, at the same background pressure, the calibration was obtained by one evaporation source at a time. Each evaporation source was calibrated at six different temperatures in the range of working temperature. The relation between the effusion cell temperature (T) and the deposition rate (r) follows the equation [54]:

$$\ln(r) = a\frac{1}{T} + b. \tag{3.14}$$

Using a least-square fit method, the parameters a and b can be determined as shown in the calibration curves of each effusion cells.

Calibration of the Cu Effusion Cell

The calibration of the Cu effusion cell is summarized in the Table 3.3 and the plot of the BEP versus the cell temperature is shown in Fig. 3.13.

Table 3.3: Calibration of the Cu effusion cell.

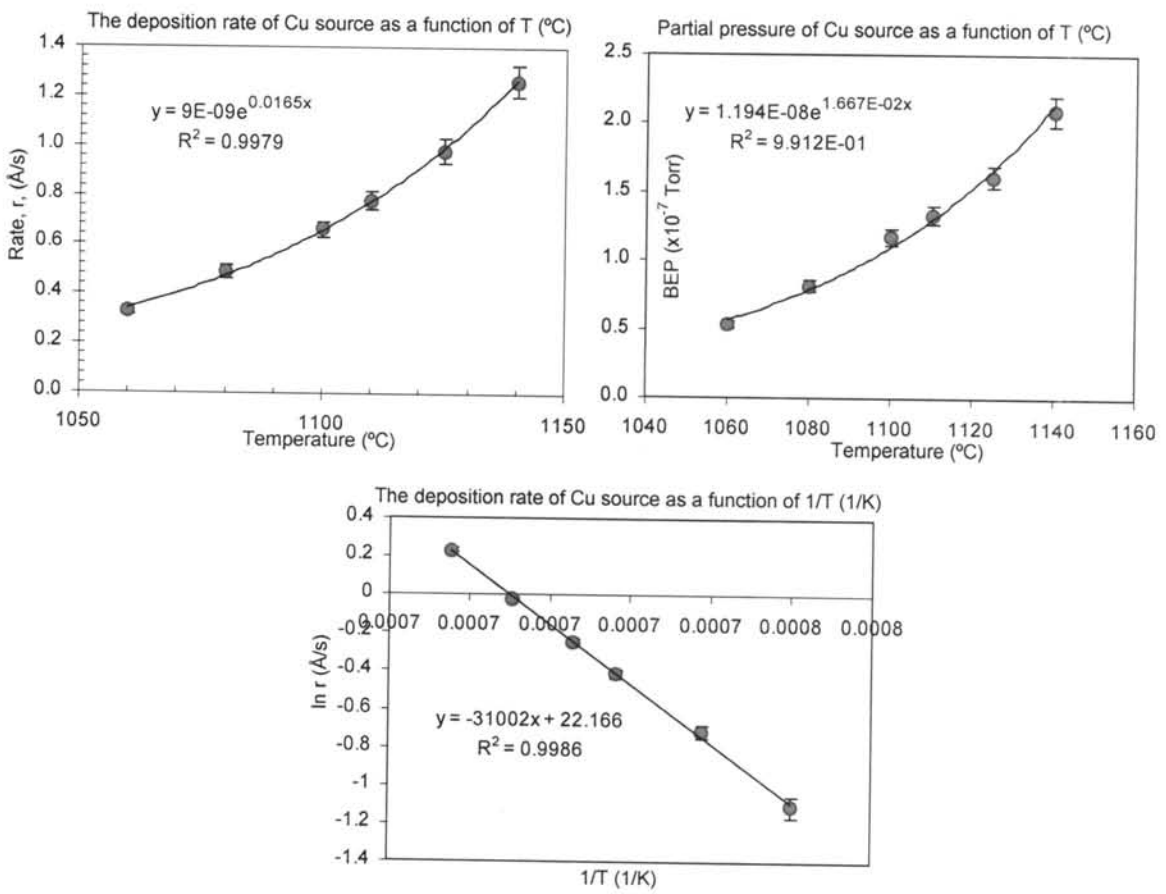| T_{Cu} (°C)	BEP (Torr)	Rate (Å/s)	Flux (1/cm^2 s)
1060	5.33×10^{-8}	0.33	2.80×10^{14}
1080	9.53×10^{-8}	0.49	4.16×10^{14}
1100	1.17×10^{-8}	0.66	5.60×10^{14}
1110	1.33×10^{-7}	0.78	6.62×10^{14}
1125	1.73×10^{-7}	0.98	8.32×10^{14}
1140	2.09×10^{-7}	1.26	1.07×10^{15}

Figure 3.13: Calibration of the Cu effusion cell.

Calibration of the In Effusion Cell

The calibration of the In effusion cell is summarized in the Table 3.4 and the plot of the BEP versus the cell temperature is shown in Fig. 3.14.

Table 3.4: Calibration of the In effusion cell.

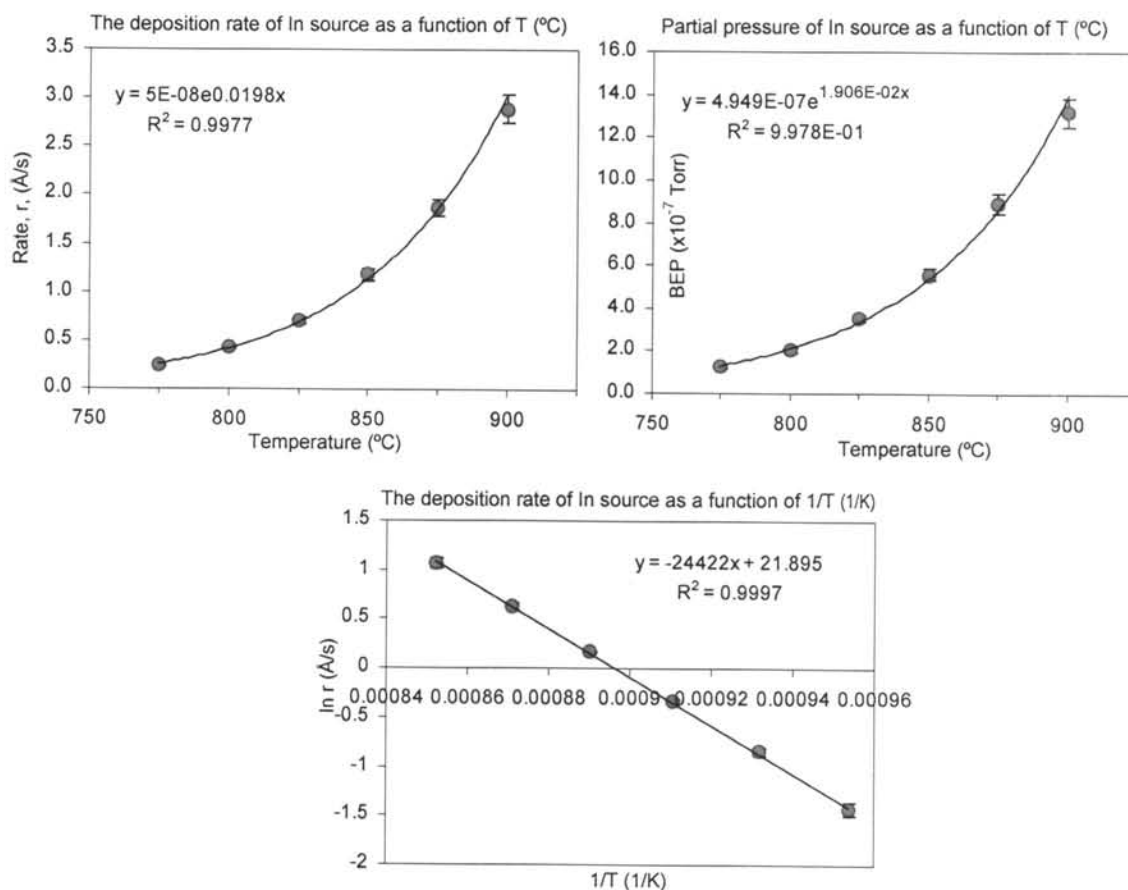| T_{In} (°C)	BEP (Torr)	Rate (Å/s)	Flux (1/cm^2 s)
775	1.25×10^{-7}	0.24	9.2×10^{13}
800	2.0×10^{-7}	0.43	1.65×10^{14}
825	3.49×10^{-7}	0.71	2.72×10^{14}
850	5.56×10^{-7}	1.18	4.52×10^{14}
875	8.90×10^{-7}	1.87	7.17×10^{14}
900	1.31×10^{-6}	2.89	1.10×10^{15}

Figure 3.14: Calibration of the In effusion cell.

Calibration of the Ga Effusion Cell

The calibration of the Ga effusion cell is summarized in the Table 3.5 and the plot of the BEP versus the cell temperature is shown in Fig. 3.15.

Table 3.5: Calibration of the Ga effusion cell.

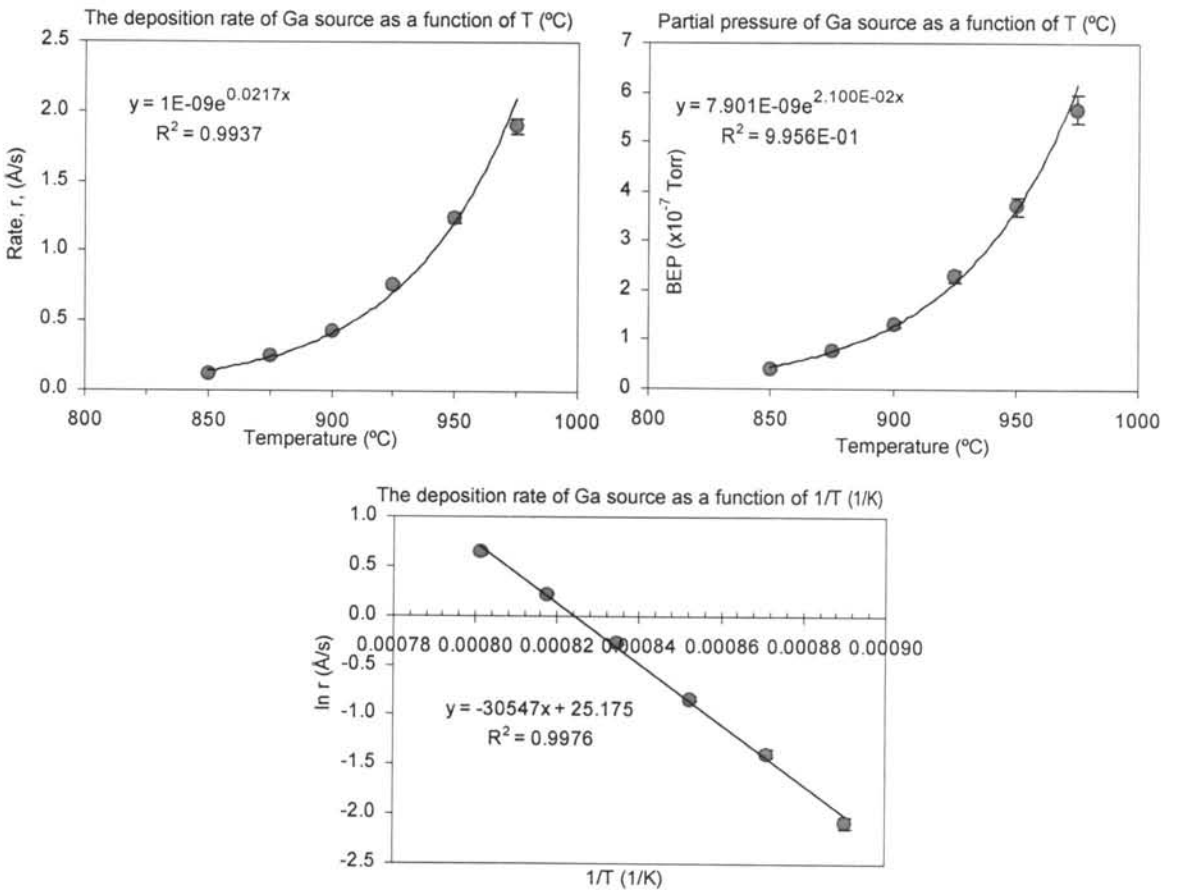| T_{Ga} (°C)	BEP (Torr)	Rate (Å/s)	Flux (1/cm^2 s)
850	4.09×10^{-8}	0.12	6.32×10^{13}
875	7.79×10^{-8}	0.25	1.27×10^{14}
900	1.33×10^{-7}	0.43	2.21×10^{14}
925	2.29×10^{-7}	0.76	3.87×10^{14}
950	3.72×10^{-7}	1.24	6.33×10^{14}
975	5.66×10^{-7}	1.89	9.67×10^{14}

Figure 3.15: Calibration of the Ga effusion cell.

Calibration of the Se Effusion Cell

The calibration of the Se effusion cell is summarized in the Table 3.6 and the plot of the BEP versus the cell temperature is shown in Fig. 3.16.

Table 3.6: Calibration of the Se effusion cell.

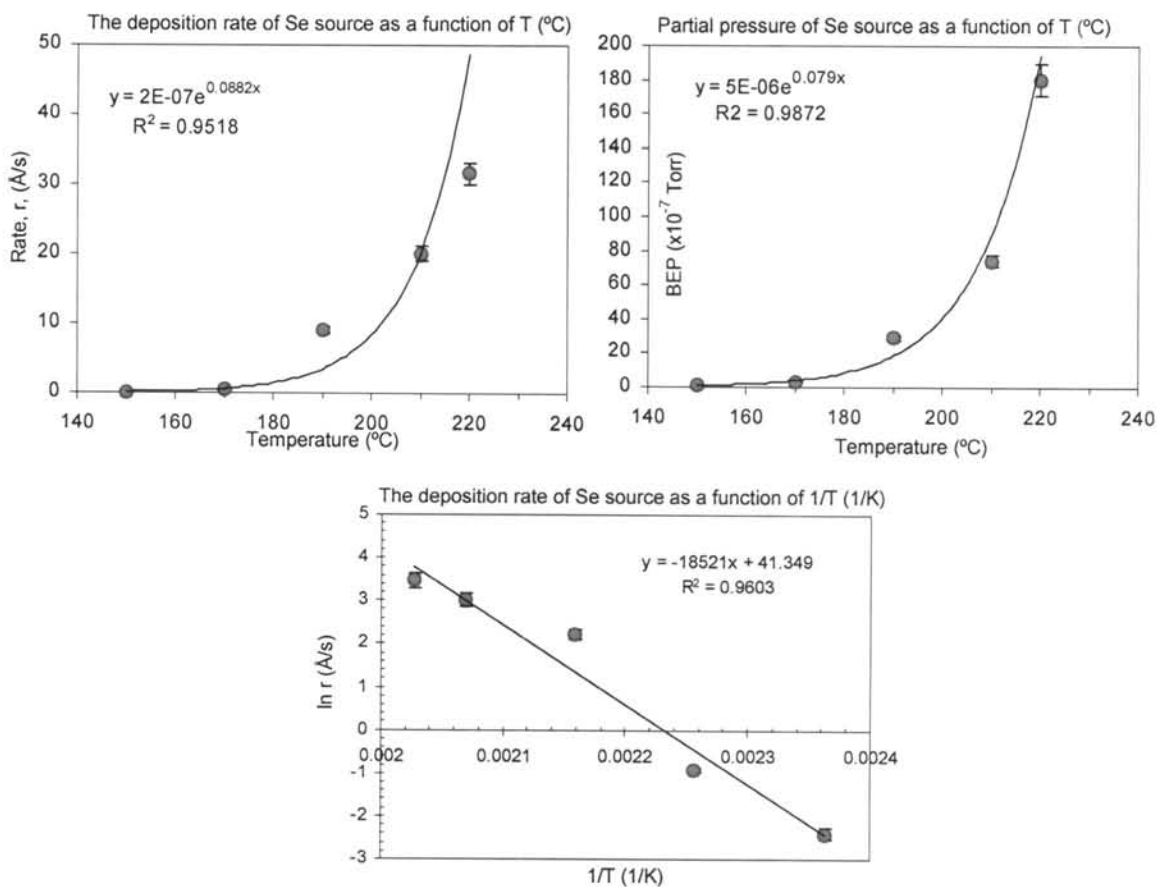| T_{Se} (°C)	BEP (Torr)	Rate (Å/s)	Flux (1/cm^2 s)
150	7.08×10^{-8}	0.09	3.28×10^{13}
170	3.32×10^{-7}	0.39	1.42×10^{14}
190	2.87×10^{-6}	9.00	3.28×10^{15}
210	7.42×10^{-6}	20.10	7.34×10^{15}
220	1.80×10^{-5}	31.60	1.15×10^{16}

Figure 3.16: Calibration of the Se effusion cell.

3.6   Conclusions

In this chapter, we have briefly described the preparations of both SLG and GaAs to be used as the substrates for growing the polycrystalline and epitaxy layer of $CuIn_{1-x}Ga_xSe_2$. The calibration of substrate temperature has also been performed to an acceptable level of accuracy using the observation of the RHEED patterns of the desorption of oxide layer at $583°C$ on the GaAs surface. We have also calibrated the beam equivalent pressures of the Cu, In, Ga and Se effusion cells as a function of temperature.